Design and demonstration of a seabird-inspired fixed-wing hybrid UAV-UUV system

To cite this article before publication: William Stewart *et al* 2018 *Bioinspir. Biomim.* in press https://doi.org/10.1088/1748-3190/aad48b

Design and Demonstration of a Seabird-Inspired Fixed-Wing Hybrid UAV-UUV System

William Stewart[1], Warren Weisler[2], Marc MacLeod[2], Thomas Powers[2], Aaron Defreitas[2], Richard Gritter[2], Mark Anderson[3], Kara Peters[2], Ashok Gopalarathnam[2], Matthew Bryant[2]

[1] North Carolina State University, Dept. of Mechanical and Aerospace Engineering, Raleigh, NC, USA Corresponding Author: wjstewa2@ncsu.edu
[2] North Carolina State University, Dept. of Mechanical and Aerospace Engineering, Raleigh, NC, USA
[3] Teledyne Scientific and Imaging, Durham, NC, USA

Abstract.

This paper looks to the natural world for solutions to many of the challenges associated with the design of fixed-wing cross-domain vehicles. One example is the common murre, a seabird that flies from nesting locations to feeding areas, dives underwater to catch prey and returns. This hunting expedition provides an outline of a possible mission for a cross-domain vehicle. While the challenges of cross-domain vehicles are many, the focus of this paper was on buoyancy management and propulsion. Potential solutions to each challenge, inspired by multiple animals that cross between aerial and underwater domains, are investigated. From these solutions, three design concepts are considered, a quadrotor/fixed-wing hybrid, a vertical takeoff and landing (VTOL) tailsitter aircraft, and a waterjet-assisted takeoff vehicle. A comparison was made between the capability of each concept to complete two missions based on the common murres' hunting expedition. As a result of this comparison, the VTOL tailsitter design was selected for further study. In-depth design was conducted and a prototype vehicle was built. The completed vehicle prototype successfully conducted submerged operation as well as four air flights. Flights consisted of egress from water, flight in air, ingress into water in each flight, and water locomotion. A total of 11 minutes, 23 seconds of flight time was recorded as well as underwater swims down to 12 ft (3.7 m) below the surface.

Keywords: multimodal locomotion, seabird, submersible aircraft, unmanned aerial-aquatic vehicle, unmanned aerial vehicle, unmanned underwater vehicle

Submitted to: *Bioinspir. Biomim.*

Introduction

The common murre, or *Uria aalge* is a diving seabird found in both the Atlantic and Pacific Oceans. The bird has a relatively large body and small wings (mass of about 946 g, wing area of about 0.053 m^2 with a wing loading of about 176 N/m^2) [1]. Murre parents breed and rear chicks on land for the first 3 weeks of the fledglings life [2]. During this time, the parent murres go on hunting expeditions to acquire food for the young bird. On a single expedition, the birds will travel up to 43 km distance, dive about five times, with dive times of up to a minute and a half, to depths of 60 m before flying back to the nest [1, 3]. This ability of the common murre to fly, complete multiple dives and return to their point of origin provides a nice example of potential missions that could be completed with the development of a new domain-transitioning vehicle concept.

Cross-domain vehicles are a new class of bioinspired vehicles [4]. The motivation for developing a hybrid underwater/aerial vehicle is to combine the speed, maneuverability, and range of an aircraft with the stealth, endurance, and subsurface sensing capabilities of a submarine. Applications of such vehicles include mobile sonobuoys, water sampling, and identification of unexploded ordinance such as naval mines. The advantage gained is that these vehicles can be used to rapidly relocate sensors and equipment during the mission. To adequately combine the capabilities of submarines and aircraft, the vehicle must be able to repeatedly complete four tasks: water egress, air flight, water ingress, and underwater locomotion, like the common murre. Individually, these capabilities are seen in other animals as well, such as penguins transitioning between water and land [5], flying fish transitioning between water and air [6], and dragon flies spending their adolescence in water and adulthood in air, returning to the water for reproduction [7]. A hybrid UAV-UUV (unmanned aerial-underwater vehicle) concept that utilizes a squid-inspired waterjet along with gannett inspired morphing wing to transition to and from water has been demonstrated by Sidall et al. [4]. Key limitations to this vehicle are that it has a one-time-use waterjet for takeoff, it has a nonconventional folding wing, and it works best on the micro air vehicle scale. More recently, Siddall and Kovac have built a prototype vehicle as well as made advances on the waterjet design [8–11].

Other examples of transitioning vehicles have also been developed over the past

few years. The U.S. Naval Research Lab has demonstrated three hybrid vehicles, Sea Robin and Test Sub. The first, Sea Robin is a single-use folding wing aircraft that is launched from a submarine torpedo tube into the air [12]. The second, Test Sub is dropped from a flying aircraft, glides in the air, lands in water, and continues its mission underwater. It is also a single-use vehicle [13]. Similarly, the third is a flapping fin vehicle that can also be dropped from an aircraft [14]. None of these designs are capable of returning to their original domain and continuing operations.

Outside the Naval Research Lab a number of theoretical studies have been conducted. The U.S. Naval Surface Warfare Center has published a study on the feasibility of a manned cross-domain vehicle [15]. This study suggests that the design approach for air-water vehicles must be dominated by the air flight requirements, and therefore be much more akin to a submerged aircraft as opposed to a flying submarine. To that end, they proposed a flying-wing configured aircraft with flooded structures, and dual propulsion systems, one for air and one for water. Crouse [16] presented similar aircraft designs after studying sizing and design space relations. All of these projects developed some working components of a vehicle, but none have built a complete cross-domain vehicle system.

A number of multirotor designs have also been investigated recently that can smoothly transition between air and underwater operations. Drews et al. [17] identified the key characteristics of airborne vehicles and submerged vehicles. Using these, they selected a quadcopter architecture and developed a simulation for the control of a small quadrotor vehicle using a PD controller [17]. Maia et al. built a tethered multirotor vehicle that was demonstrated operating both underwater and in the air [18]. This team was able to demonstrate transition between domains, multi-domain propulsion, and merging requirements for aerodynamic parameters and hydrodynamic parameters. This prototype demonstrates all aspects of the hybrid aerial and underwater operation, however it does so with a rotary-wing configuration, making it less efficient than a fixed-wing aircraft while in air.

The goals for this research were to design, build, and operate a fixed-wing vehicle capable of completing a mission similar to that of the common murres hunting expeditions. That is, the vehicle should be able to achieve controlled locomotion in both air and water as well as repeated transitions between the two domains. To aid in the design process, vehicle subsystem concepts of operation are borrowed from many different sources in the natural world. Unlike previous cross-domain fixed-wing examples, this vehicle must to be able to complete multiple full cycles between

water and air. This prototype vehicle is not intended to be an optimized design, but rather a proof of concept demonstration that can complete all four of the tasks defined previously. Vehicle scale was not limited to the size of the murres, however the ability to scale to match future needs was a requirement. The same was true of aircraft performance metrics such as range, endurance, operating speeds, and service ceilings.

Design Considerations

This section introduces two of the key challenges associated with UAV-UUV hybrid vehicle development. Potential solutions are discussed and compared for both of the challenges. Design advantages and tradeoffs are investigated.

Depth Management

One of the main challenges facing the design of UAV-UUV hybrids is buoyancy. This is especially true of high-volume structures such as wings. Figure 1(a) shows that increasing the chord length of the wing for the same airfoil section causes the buoyancy force per unit span to increase quadratically, presenting a challenge for the vehicle to maintain depth underwater.

There are two strategies employed by seabirds to control depth while underwater. The first is by using muscles to squeeze the air in their lungs to a smaller volume [19]. Compressing the air increases the overall density of the bird causing it to sink, whereas relaxing the muscles and allowing the gas to expand increases the bird's volume, increasing buoyancy causing the bird to float back to the surface. A human-made variable buoyancy system (VBS) which was presented by MacLeod and Bryant [20], has demonstrated a similar process of compressing air to change buoyancy. With this device, net vehicle buoyancy is decreased by pumping ambient water into a rigid, compressed-air-filled pressure vessel, increasing the weight of the vehicle and further compressing the air inside. To increase net buoyancy, a vent valve is opened, allowing the internal pressure to expel the ballast water, while the compressed air is held captive by an elastomer membrane. Figure 1(b) shows the VBS sizing requirements as a function of vehicle parameters. Changing the vehicle volume or mass changes the fraction of the vehicle volume that the VBS must be able to flood to achieve neutral buoyancy. The inherent advantage to the VBS is that it

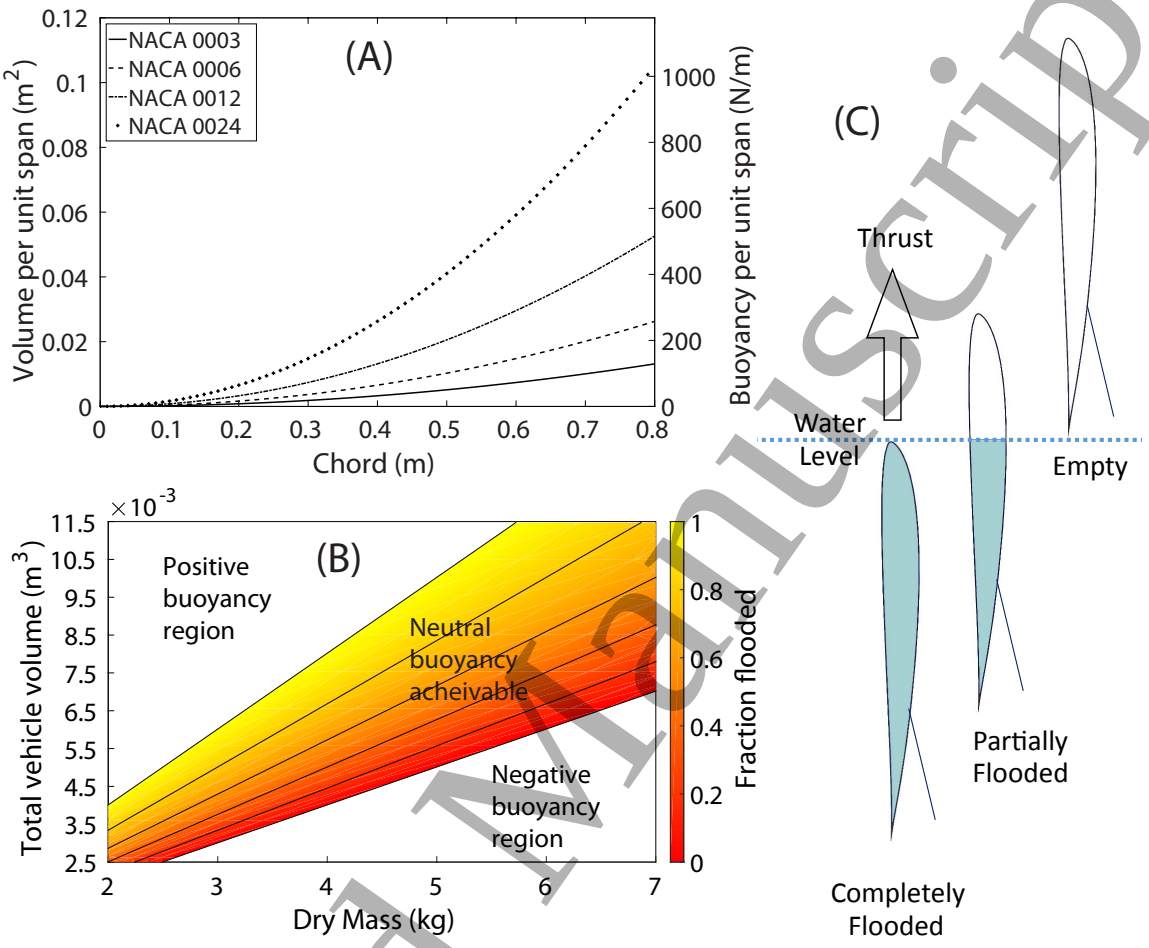

Figure 1. (a) Buoyancy scaling per unit span for various NACA airfoil shaped volumes. (b) VBS system sizing as a function of dry vehicle weight, volume, and fraction flooded. Black lines indicate lines of constant fraction flooded corresponding to values indicated on the right. (c) Passively draining wing diagram.

enables fine tuning the buoyancy throughout the duration of the mission, allowing the vehicle to adapt to changing environments and use the system to change depth. The main drawback is the additional weight and energy consumption of the system pump and valves.

The second strategy used to control depth by seabirds such as the common murre is to actively swim downwards [21]. This is a particularly attractive option

for animals that make the transition between domains, but spend the majority of their time in air, requiring a design favoring flight over swimming. Analogously, this strategy could be best suited for a vehicle that focuses on air operations, with a minority of time and energy spent below the water surface. From the engineering vantage point, this is a strategy of generating a downward lift force. A simple way to accomplish this is to turn the vehicle (and therefore it's lifting surfaces) upside down. The advantage to this is that it can be achieved without physical modifications or additions to the vehicle. The whiffling geese perform a similar aerodynamic maneuver whereby they flip themselves upside down, reversing the direction of the lift vector from their wings [22]. An alternative solution is to modify the camber or angle of attack of the lifting surfaces. A simple implementation of such a strategy is the use of flapperons, which are control surfaces similar to ailerons, however, the control surfaces on both sides of the wing are capable of deflection in the same direction. A final option is to use propellor thrust to simply push the vehicle downward. The use of downward lift is an active depth control method. As such it has intrinsic energy requirements and reduces the loiter capability of the vehicle.

Typically, the largest empty volume on a fixed-wing aircraft is the wing. This is a result of designs driven by the need for high lift, light weight structures. A large share of the buoyancy challenge encountered by fixed-wing hybrid UAV-UUVs stems from large wing volumes. One way to alleviate the buoyancy induced by wing structures is to flood the structures with water upon ingress and drain them on egress. Doing this requires, as completely as possible, ingesting and expelling water. While this is achievable with a system similar to the VBS, being able to flood and drain the wing passively would be advantageous. Once again, nature offers a potential solution. Duck (biological family *Anatidae*) feathers and the leaves of the lotus plant have a hydrophobic coating enabling them to shed water [23, 24]. Likewise, the internal surfaces of passively flooding and draining structures can be covered in a hydrophobic coating to improve water shedding at takeoff. On a hybrid UAV-UUV, water floods the wing due to ambient hydrostatic pressure when vent ports are opened as the vehicle enters the water. Similarly, water drains through the vents during egress when the propulsion system lifts a portion of the wing above the surface as illustrated in figure 1(c). Takeoff for a vehicle that utilizes this kind of passive draining should be vertical. This is because the vertical orientation gives the largest outlet area for water to drain during takeoff. The vents could be spoileron control surfaces which allow for dual use of the structure. The internal structure

in the wing can be designed using trusses to allow water to easily flow throughout the wing structure and prevent it from being trapped inside. Wet compartments, either on the wing or fuselage, that house sensors, motors, and antennas can use the same combination of vents and water outlets to flood and drain. The more wet compartments on board, the less dry volume the vehicle will have, reducing its overall buoyancy. This wing design scales well because increasing the span does not increase the water volume per water outlet area ratio. The downside to this design is that the buoyancy cannot be actively tuned for different environmental conditions.

Propulsion for Egress and Cruise

The takeoff transition represents one of the most difficult tasks for a UAV-UUV hybrid vehicle. This is due to the energy requirements involved in building up adequate takeoff speed in a dense fluid such as water. As a result, the choice of propulsion system represents a critical design decision.

Challenges stem from differences in propeller design for water and air. Small unmanned aircraft usually employ large diameter, lightweight, wood, carbon, or polymer propellers. Watercraft on the other hand employ non-corrosive metallic propellers with comparatively small diameters. Water propeller design is driven in large part by reducing cavitation, a problem not seen by aircraft propellers. The result is that a propeller designed to work well in one domain will be considerably less efficient in the other.

Electric motors lend themselves well to UAV-UUV designs. Brushless motors have been demonstrated to work while submerged in water [13]. This allows them to be placed outside the dry compartment, enabling more freedom in motor configuration. One possible configuration is to have a single electric motor and propeller for use in water and air. This dual use strategy is quite common in the natural world, examples include webbed feet that enable swimming in water and walking on ground [21], squids that use their tentacles for control in the air and underwater [25] and large variable camber fins on flying fish that are used to maneuver underwater and glide in the air [6]. The drawback is an inherent efficiency compromise due to having suboptimal tuning in one or both domains. For instance, as agile as penguins are in the water, they accept a performance penalty in their gait while on land. When compared with a mammal of the same mass, it costs a penguins about 60% more energy to run on land, and 10% less energy to swim underwater.

This is an acceptable tradeoff as they spend most of their time in the water, and don't require as much agility on land [5]. In order to overcome inefficiencies in one or the other domains, a morphing propeller could be used to modify propeller span. Morphing propellers are a relatively new technology, and so come with the associated risks. A patent for variable span helicopter blades has been filed [26]. An alternative to the morphing propellers is to use a gearbox to enable more efficient underwater water operation of an electric motor selected for air propulsion. This strategy has been successfully demonstrated on a small electric hybrid UAV-UUV [27].

Another possible configuration is to expand the single motor and propeller configuration into two separate motors and propellers. One motor-propeller pair is tuned for use in the air, and the other in the water. The easiest way to implement this is to have one motor in front of the vehicle acting as a tractor and the other in the back acting as a pusher. Both motors are sized to work well in their respective domains giving increased efficiency. Many animals use this strategy, such as birds that will fly or glide using wings, but then swim and walk on the ground with webbed feet. Squids have been shown to use their fins for propulsion in water and rapidly expel water for thrust in air [25]. When applied to a man-made vehicle, the inherent drawback is the additional weight and complexity of having two motors, two propellers, and two electronic speed controllers (ESCs).

The last electric motor configuration considered is many smaller sized motors. This strategy could be implemented on a fixed-wing vehicle in a number of different ways, from multiple forward facing, wing mounted electric motors, to a combination fixed-wing multirotor vehicle. Thrust vectoring could be accomplished by orienting the motors in different directions, which could help with vehicle control on takeoff.

Taking cues from squid, the last propulsion system considered is a waterjet device for egress. This is the strategy favored by Sidall and Kovac [4]. For this subsystem, a modification to the VBS proposed by MacLeod and Bryant [20] to enable it to be used to generate a rapid burst of thrust is considered. Using a quick-exhaust valve, air pressure can eject the water from the VBS tanks backwards and propel the vehicle into the air from the water surface. A diagram of the device is shown in figure 2(a). The waterjet egress would be used to reduce the power requirements on the electric propulsion system of the aircraft. The advantages to this approach is that it is a minor modification to a system already considered for buoyancy control and that it takes advantage of the surrounding environment to operate. Figure 2(b) shows the energy required for this system to reach the pressure

needed to takeoff using the waterjet egress method. The higher the pressure required to takeoff, the more energy that is required to prime the waterjet for takeoff. The pressure requirements were calculated for 2 through 6 L tank sizes. These size tanks roughly correspond to the scale of interest for this study. The pumping energy was calculated using relationships defined in the datasheets for a small commercially available pump, the Hydro Leduc PB33.5, using the model presented by MacLeod and Bryant [20]. These energy estimates were calculated using the model presented and discussed in the modeling section. Of interest here is that at a lower vehicle mass, a smaller tank is more efficient, but as the vehicle mass increases, it becomes more efficient to use a larger tank. Thus, there is an optimal tank size for a given vehicle mass. One downside to this design is that the vehicle will require other propulsion systems for locomotion in air and water.

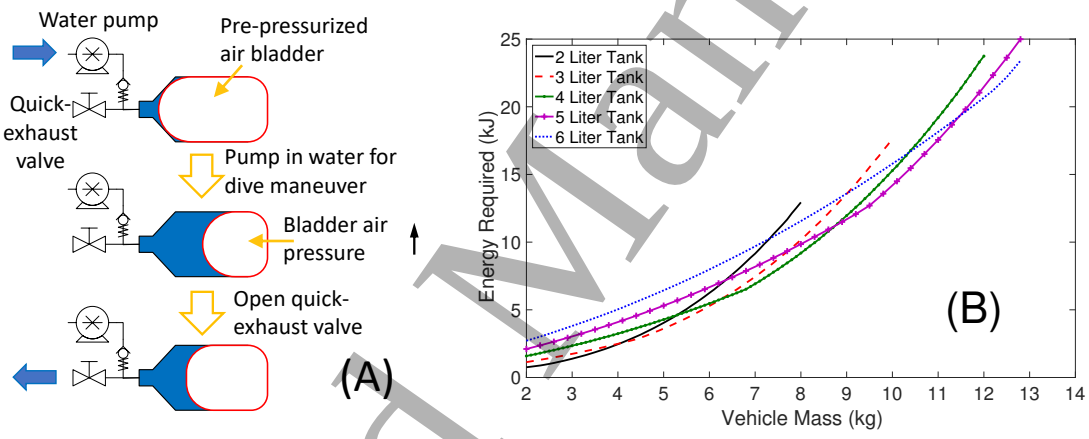

Figure 2. (a) Diagram of waterjet propulsion system, the blue areas indicate the water-filled portion of the tanks, the white areas indicate air. (b) Waterjet takeoff energy requirements as a function of vehicle weight.

This work only considers waterjet systems charged by an electric motor due to their being readily realized at the vehicle scales of interest, however, other methods of pressurizing a waterjet exists. One way this could be achieved is by using electrolytic plates to convert split water into oxygen and hydrogen. Recently, this method of egress was successfully demonstrated on a hybrid aerial-aquatic microrobot [28]. Another pressurizing technique is to use explosive solid fuel to propel water out of the device. A recent example is demonstrated by Siddall et al using CaC_2 as the

fuel [29].

Representative Hybrid UAV-UUV Missions

Using the murres' hunting expeditions as a template, two representative mission profiles for a hybrid UAV-UUV were defined. Just as the murres travel first to feeding areas, both missions begin with a 5 mile (8.0 km) flight to the mission area of interest. Mission 1, illustrated in figure 3, then puts an emphasis on the air domain. This mission assumes that travel between multiple ingress points is performed in the air domain. The mission consists of three transitions to and from underwater operations without any travel underwater. Mission 2, also illustrated in figure 3, places more emphasis on underwater operations with fewer transitions between domains. These two mission profiles can be used to determine if a single vehicle concept could perform well in both domains, or whether two radically different designs would be needed for missions focused primarily on air travel or water travel scenarios.

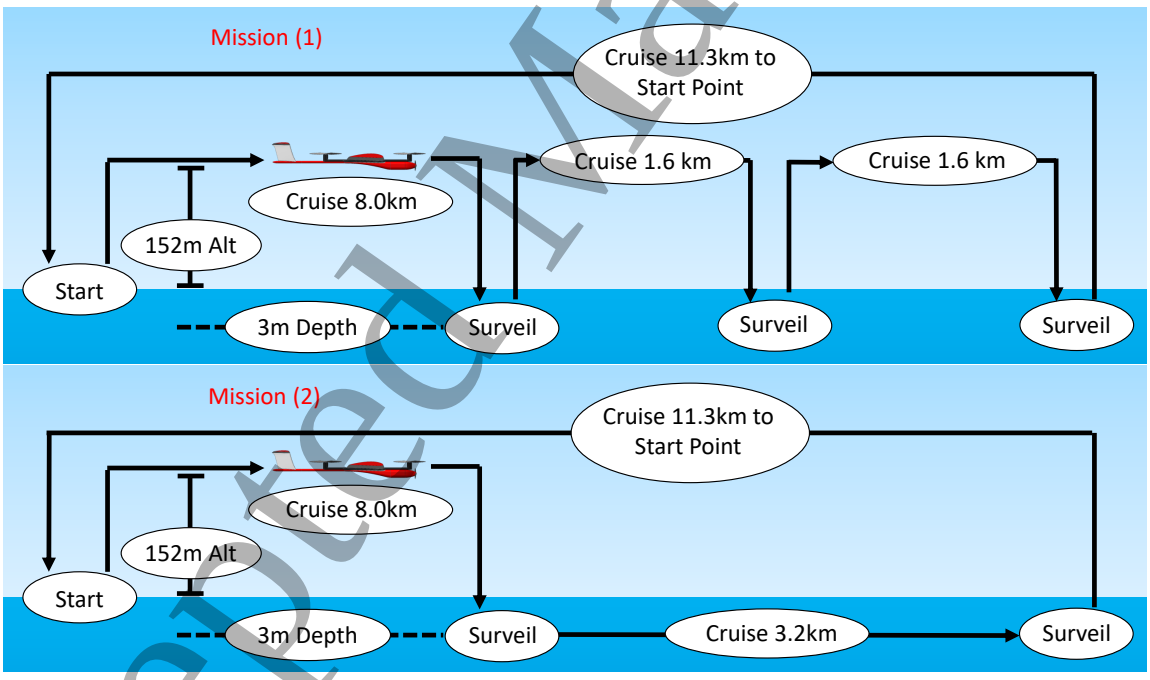

Figure 3. Mission profiles considered for comparison of candidate vehicle designs.

Vehicle Concepts

The solutions discussed in the previous section are combined into the three operational concepts described in this section. Each concept is based on a fixed-wing vehicle design due to the increased efficiency in air travel. All of the design concepts are assumed to be able to maintain neutral buoyancy passively, however the concepts vary in the propulsion mechanism and in how they change depth.

Quadrotor Fixed-Wing Hybrid Vehicle Concept

The first concept considered is a quadrotor-fixed-wing hybrid aircraft. This configuration combines the multiple small electric motors for propulsion with the active negative lift depth control, by way of using it's vertically oriented electric motors. As a result, the vehicle is designed to be neutrally buoyant for a given mission. Figure 4 shows the concept of operations for this configuration. The vehicle is a conventionally configured airplane with pylons mounted under the wing to support vertically oriented electric motors on each end. There are also two small electric motors, one forward facing and one aft facing, used for forward thrust in air and water respectively. To land, the vehicle transitions from horizontal flight into a hover by engaging the vertically-oriented motors and reducing forward speed. The vehicle then slowly lowers itself into the water. Underwater, the vehicle regulates its depth using the vertically-oriented motors. It maneuvers horizontally with the small aft-facing electric motor in the tail of the aircraft. The vehicle surfaces using the vertical motors and continues up into the air where it transitions back into forward flight by engaging the forward-facing electric motor and building up horizontal speed. This configuration thus aims to combine the attributes of a quadrotor and a fixed-wing aircraft. The vehicle has simple geometry and can take off vertically. Additionally, the aircraft takes advantage of the efficiency of a fixed-wing vehicle in forward flight. The disadvantages come in the form of added weight as it is carrying the components of two vehicles in one. The vertical takeoff occurs in an orientation that produces significant drag as compared with forward flight. Latitude Engineering has built a flight-only vehicle that operates in a similar manner [30].

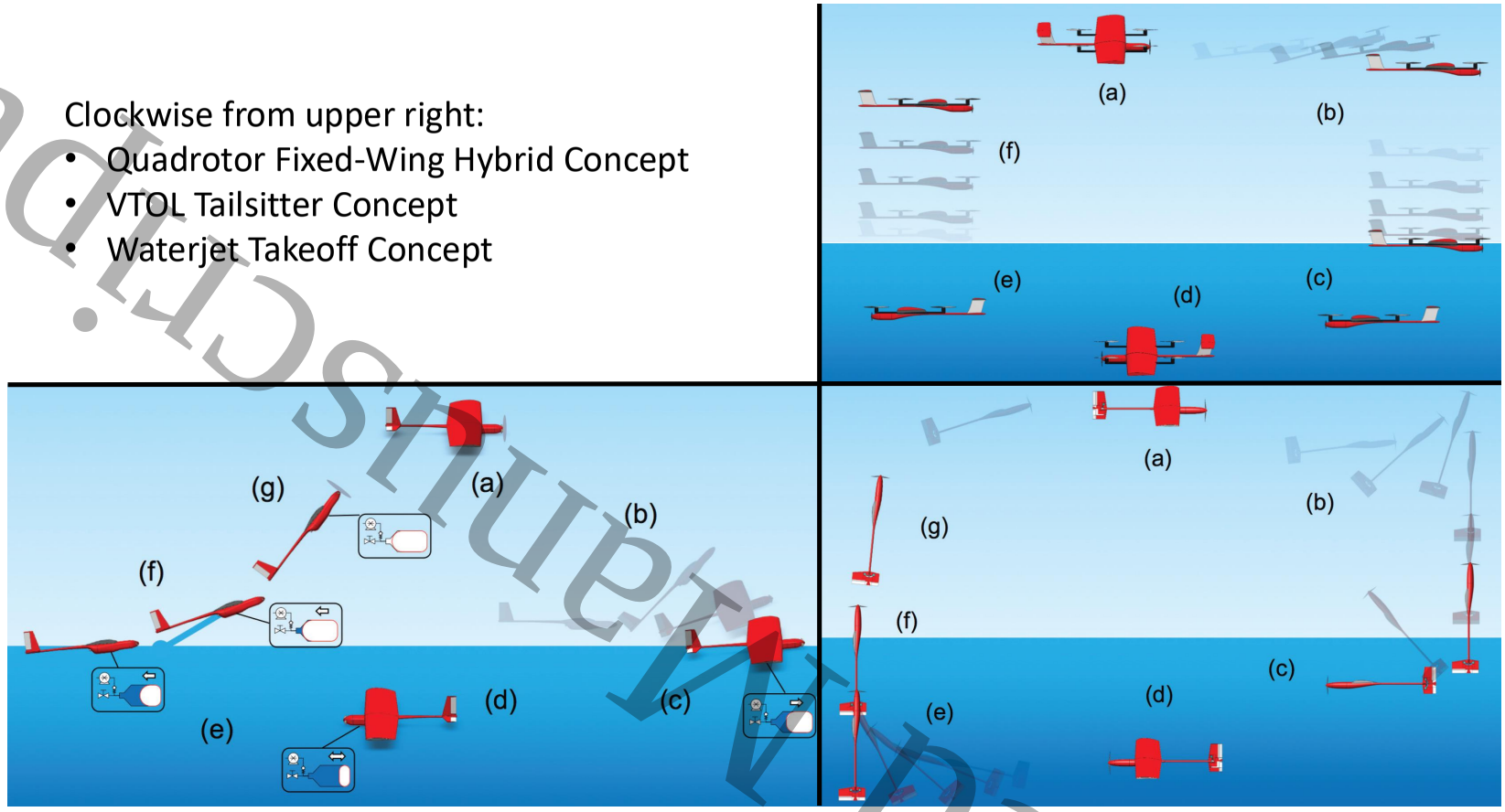

Figure 4. Quadrotor hybrid vehicle concept operation stages: (a) Forward flight mode, with a front-facing motor engaged, lift produced by wings. (b) Transition to vertical flight by engaging vertically-oriented motors. (c) Submergence using vertically-oriented motors. (d) Depth regulated by vertical thrust. (e) Surfacing via vertical thrust. (f) Traditional multicopter vertical takeoff. **VTOL tailsitter vehicle concept operation stages:** (a) Conventional fixed-wing flight. (b) Pitch up to vertical hover enabled by high thrust-to-weight ratio. (c) Touchdown in water and submergence via neutral buoyancy and control surfaces. (d) Underwater maneuvering enabled by water motor. (e) Pitch up to vertical orientation. (f) Optional ballast tanks drained, water and air propellers engaged for egress. (g) Water prop disengaged, climb and pitch down to forward flight. **Waterjet-assisted takeoff vehicle concept operation stages:** (a) Conventional fixed-wing flight. (b) Stall-splash to reduce speed and gently drop into water. (c) Active submergence by pumping water into pressurized storage tank. (d) Water propeller used for locomotion. (e) Vehicle made positively buoyant to float on surface. (f) Quick expulsion of water from buoyancy tank used to takeoff. (g) Air propeller used to transition from takeoff to forward flight.

VTOL Tailsitter Vehicle Concept

The second concept is a VTOL (vertical takeoff and landing) tailsitter aircraft configuration, as shown in figure 4. This concept combines the two electric motor configuration for propulsion with the passively draining wing to reduce buoyancy as well as deflecting control surfaces to swim downwards. When in the air, this concept uses a single large electric motor to generate a thrust to weight ratio that is greater than one. The vehicle is conventionally configured and moves through the air as a typical fixed-wing airplane. During the transition from flight to water operations, the aircraft conducts a pitch-up maneuver to orient itself vertically. It then reduces thrust to lower itself into the water. When underwater, the vehicle can maneuver in the same manner as it does in the air, using propeller thrust and flow over control surfaces to generate control forces. To generate thrust underwater, the vehicle uses a second, smaller electric motor with a propeller designed for in-water use. When transitioning from underwater operation to air flight, the vehicle uses the same pitch-up maneuver to orient itself vertically at the surface, and uses both its air motor and water motor to lift itself out of the water. This concept aims to combine the advantages of a vertical takeoff and horizontal flight from the quadrotor hybrid without the disadvantages of the high-drag horizontal takeoff orientation and weight of additional motors. The disadvantage is a reduction in efficiency due to disparate propeller matching requirements of vertical hovering and cruise flight. A similar flight-only vehicle is the Aerovel Flexrotor [31].

Waterjet Takeoff Vehicle Concept

The third concept is a waterjet-assisted takeoff vehicle illustrated in figure 4. This concept combines dual electric motors for propulsion and the active VBS for depth control. In addition, this vehicle uses a waterjet for propulsion during takeoff. The vehicle operates in the same manner as the VTOL operation concept except that it uses pressurized water to propel itself out of the water and into the air. The pressurized water is also used during underwater operation as a means of depth regulation. During landing, the vehicle performs a stall-splash maneuver. To do this the vehicle reduces altitude and forward speed. It flares just before landing to bleed off as much forward speed as possible and drops into the water. The wing used here is a fully sealed semi-monocoque design. Unlike the VTOL tailsitter, this design has a thrust to weight ratio of less than 1, as a result of which it cannot lower itself

into the water vertically. This concept seeks to alleviate the hover/cruise propeller design mismatch of the tailsitter concept by adding an additional mechanism for egress thrust. As with other designs, while underwater, the vehicle achieves forward motion using a small water propeller in the tail of the aircraft. Because the air motor/propeller is not responsible for generating all the takeoff thrust on its own, it can be sized for cruise flight. The disadvantages to this concept are in the added weight and energy required for the waterjet subsystem due to the need for a pressure vessel and pumps. This is a similar solution to the vehicle developed by Siddall and Kovac, but we account for the components and energy required to repeatedly pressurize the water tank onboard [8].

Modeling

To compare the performance of each vehicle concept in completing the representative missions, estimates of vehicle performance characteristics were calculated. Each concept is designed to be passively neutrally buoyant once landed as well as have the same base fixed-wing airframe weight. The estimate for that airframe based on structural components and construction methods was 8.7 lbs (38.6 N). The differences in total vehicle weight from design to design are based on differing weights of propulsion systems and associated structure. Component-wise, the VTOL Tailsitter is the simplest concept. Table 1 shows the component weight buildup for the VTOL Tailsitter. This buildup includes the air motor, propeller, and ESC as well as the water motor, propeller, and ESC. The total component weight is listed as 1.91 lbs (8.51 N) meaning that the total aircraft weight is about 10.7 lbs (47.4 N). Component weight buildups were used to estimate the additional weight for the VBS and the waterjet system as well as the quadrotor motors and associated structure.

Drag coefficients for each concept were calculated based on a drag buildup. The drag buildup took into account lifting-surface induced drag from AVL [32], lifting-surface profile drag from XFOIL [33], laminar flat-plate drag for the tail [34], and profile drag for the fuselage. Tail drag and fuselage drag were estimated using values from Hoerner [35]. $C_{D_{vert}}$ refers to the coefficient of drag when egressing or ingressing, which differs from normal operations for some concepts.

Launch energy was calculated using a MATLAB simulation of takeoff. While submerged, this simulation incorporated thrust from the water propellers, water-based drag, hydrodynamic added mass, and vehicle weight. When transitioning

Table 1. Component weight buildup for the propulsion system of the VTOL tailsitter

Component	Weight (N)	Weight (lbs)
Hacker A50-12L Motor	4.36	0.981
Castle Edge 100 Lite ESC	0.5494	0.1235
APC 17x10 Propeller	0.663	0.149
Hacker A40-14S Motor	2.04	0.459
Castle Edge 100 Lite ESC	0.5494	0.1235
APC 14x10 Propeller	0.3531	0.0794
Total	8.51	1.91

to air, the simulation also accounted for the air propellers, air-based drag, and weight of the vehicle. The simulation considers each of the vehicles as a point mass and therefore does not account for multiphase flows. To accurately predict the takeoff trajectory of a vehicle a multiphase flow model would be needed, however this analysis is simply comparing vehicle concepts. Current work in progress that will be presented in Stewart et al. will account for these multiphase flow effects [36]. For ease of comparison, the egress trajectories for the VTOL tailsitter and waterjet were assumed vertical. The waterjet concept makes use of its water and air motors in addition to the waterjet device on takeoff. In this analysis, wing draining for the VTOL tailsitter concept was assumed to occur fast enough that it does not have an effect on takeoff performance. The quadrotor hybrid concept accounted for a transition between vertical velocity and horizontal velocity. This was done because unlike the other concepts, the quadrotor hybrid vehicle retains a horizontal orientation throughout its takeoff.

Takeoff energy required for the waterjet device was calculated using the following equation,

$$\mathrm{E}_{\mathrm{waterjet}} = \int_{V_0}^{V_f} \frac{V_0 p_0}{V_f} \mathrm{d}V \tag{1}$$

where, V_0 is the initial air volume in the waterjet tank, V_f is the final air volume in the tank, and p_0 is the initial pressure in the tank. Equation 1 assumes the pump is ideal and that all input energy is converted to tank pressure. The required initial

pressure was found by iteratively solving for the starting tank pressures required for the vehicle to reach takeoff speed. The final volume is the volume of the tank due to the assumption that all the water has been ejected. Takeoff speed was defined as

$$U_{takeoff} = 1.2U_{stall} = \sqrt{\frac{2Mg}{\rho_a S C_L}} \tag{2}$$

where U_{stall} is the stall speed, M is the vehicle mass as well as any water in the tank, g is the acceleration due to gravity, ρ_a is air density, S is the wing planform area, and C_L is the lift coefficient. Lift coefficient was set to 1 for this calculation. The kinetics of the waterjet takeoff were modeled using Newton's second law in the vertical direction,

$$(M_a + M)\dot{U} = T_w + T_a + T_{waterjet} - Mg - D \tag{3}$$

where, M_a is the hydrodynamic added mass of the vehicle, $\dot{U}$ is the vertical vehicle acceleration, T_w and T_a are the thrust from the water motor and air motor respectively. $T_{waterjet}$ is the thrust produced by the waterjet device, and D is vehicle drag. Drag was calculated using the following equation,

$$D = C_D {}^1\!/_2 \rho U^2 S \tag{4}$$

where, C_D is the vehicle drag coefficient, ρ is the fluid density, air or water, and U is the vehicle velocity. Thrust from the water and air motors were calculated using,

$$T = \left[P_a({}^1\!/_2)\sqrt{2\rho A}\right]^{2/3} \tag{5}$$

where, P_a is the power available and A is the propeller disk area. Thrust for the waterjet device was calculated using equations 6 and 7, which come from Siddall et al. [4],

$$T_{waterjet} = \frac{2A_0\mu(P_{gas} - P_{atm})}{1 - \left({}^{A_0}\!/_{A_i}\right)^2} \tag{6}$$

$$\dot{M} = -\rho_w A_0 \sqrt{\frac{2\mu(P_{gas} - P_{atm})}{\rho_w\left[1 - \left({}^{A_0}\!/_{A_i}\right)^2\right]}} \tag{7}$$

where, P_{gas} is internal air pressure, P_{atm} is atmospheric pressure, A_0 and A_i are nozzle outlet area and inlet area respectively, $\dot{M}$ is the rate of change in mass of

water in the waterjet tank, ρ_w is water density, and μ is an efficiency factor. Based on work from Siddall et al, μ was set to 0.89. The equation for $\dot{M}$ was used to track the amount of water in the tank throughout the takeoff simulation. The ODE in equation 3 was solved using the boundary conditions of zero initial velocity and $U_{takeoff}$ as the final velocity. To calculate the energy curves in figure 2(b) the above model was used, however, T_w and T_a were set to 0 in equation 3. This was done to simulate takeoff with just a waterjet device and compare various tank sizes and vehicle mass. The same start and end conditions (zero initial velocity and $U_{takeoff}$) were used for this simulation as well.

Modified forms of equation 3 were used to simulate the takeoff of the VTOL tailsitter and quadrotor hybrid. For the VTOL tailsitter concept, shown in equation 8, the thrust due to waterjet device was removed. In addition to removing the thrust from the waterjet, the equation used for the quadrotor hybrid concept includes a lift term due to it's horizontal velocity as well as replacing T_w with thrust from the vertically oriented motors, T_q. To account for the horizontal velocity, the equation of motion is split into two equations, one for the vertical direction, and one for the horizontal direction. The quadrotor hybrid takeoff equations of motion for vertical and horizontal direction are given as equations 9 and 10 respectively.

$$(M_a + M)\dot{U} = T_w + T_a - Mg - D \tag{8}$$

$$(M_a + M)\dot{U}_v = T_q + L - Mg - D_v \tag{9}$$

$$(M_a + M)\dot{U}_h = T_a - D_h \tag{10}$$

Lift, L, is calculated using equation 4 and substituting a lift coefficient of 1 for C_D. The subscripts v and h indicate components in the vertical and horizontal directions respectively. The same boundary conditions of $U = 0$ to $U = U_{takeoff}$ were used for these concepts.

Cruise power required terms were calculated using drag and velocity for both water and air. Equation 11 shows the relation used,

$$P_{cruise} = DU \tag{11}$$

Cruise values underwater were calculated at a speed of 3 mph (1.3 m/s) and in air at 60 mph (27 m/s). The power required for cruise was then used to calculate the amount of energy required for each mission based on the amount of cruise time in each domain.

The energy required for landing the VTOL tailsitter and quadrotor concepts was calculated based on the thrust required to vertically lower the vehicles 30 ft (9.1 m) to the water surface at a constant rate of 5 ft/s (1.52 m/s). Landing energy for the waterjet concept was set to zero to represent the concept turning off the motor and gliding to the water surface.

To achieve neutral buoyancy once landed, the waterjet concept must first pump water into the VBS tank to change from positive buoyancy to neutral buoyancy. By continuing to pump in water this concept can then submerge below the surface. The energy required to reach a depth of 10ft (3.0m) must therefore include the energy to reach neutral buoyancy and the energy to reach a desired negative buoyancy. Submergence energy was calculated for the VBS using the following equation for a positive displacement pump,

$$\mathrm{E_{VBS}} = \int_{\theta_1}^{\theta_2} \tau \mathrm{d}\theta = \int_{\theta_1}^{\theta_2} \frac{P * \delta}{2\pi} \mathrm{d}\theta \tag{12}$$

where, τ is pump torque, θ is pump shaft angular position, P is water tank pressure, and δ is pump displacement per revolution. This equation was applied for the case of the vehicle becoming neutrally buoyant and then descending to a depth of 10 ft (3.0 m), as described in the representative missions. The required air volume change to produce a steady descent velocity of 3 mph (1.34 m/s) was used. The isentropic equation of state was used to calculate the tank pressure corresponding to the air volume change. The energy required to vent water from the VBS for surfacing using a spool valve and servo-motor was assumed to be negligible. Details of VBS performance can be found in [20].

A change of 10 ft (3.0 m) at 3 mph (1.34 m/s) was used to calculate the energy required for the other design concepts as well. The VTOL tailsitter and quadrotor hybrid concepts use forward motion to change depth, so their required energy was calculated using the cruise power required equation. As a result of assumed neutral buoyancy, ascent energy for all three concepts were the same as the descent values.

It should be noted here that the waterjet concept does not necessarily need to use the VBS to descend or ascend, and could swim downward the way the other concepts can. However, by considering the VBS technique for descent and ascent it is possible to compare the use of a VBS with swimming downward.

Results and Selected Vehicle

The concept characteristics and performance parameters resulting from the preceding analysis are shown in table 2. The performance of each concept was scored based on the energy required for it to complete each of the representative mission profiles. These scores were normalized for each mission and total score was then calculated as the sum of the normalized scores. Table 3 shows the mission scores. These scores are normalized based on the best scoring design. The analysis showed that multiple design concepts can perform well in both domains. The concept that performed best was the VTOL tailsitter aircraft. The VTOL tailsitter used the least energy because it minimizes its drag during all phases of the mission. This concept is also the simplest and lowest weight requiring fewer subsystems and points of failure.

Table 2. Concept Characteristics and Performance

Characteristics	Waterjet	VTOL Tailsitter	Quadrotor Hybrid	Units
Weight	58.1	47.4	55.8	N
$C_{D\text{air}}$	0.0185	0.0173	0.0289	N/A
$C_{D\text{water}}$	0.0142	0.0129	0.0246	N/A
$C_{D\text{vert}}$	0.0185	0.0173	1.683	N/A

Performance	Waterjet	VTOL Tailsitter	Quadrotor Hybrid	Units
Launch : 0 m/s to $U_{takeoff}$				
Energy	1.44	0.76	0.75	W-Hr
Cruise Power :				
Air, 60 mph (27 m/s)	76.33	71.38	119.2	W
Water, 3 mph (1.3 m/s)	3.803	3.277	8.010	W
Landing : 30 ft to 0 ft (9.1 m to 0 m)				
Energy	0.00	0.10	0.12	W-Hr
Depth Change : 0 ft to -10 ft to 0 ft(0 m to -3.0 m to 0 m)				
Energy per cycle	0.080	0.003	0.006	W-Hr

Table 3. Concept Mission Scores

	Waterjet	VTOL Tailsitter	Quadrotor Hybrid	Units
Mission 1 Energy	25.1	20.1	32.3	W-Hr
Normalized Rank	0.80	1.00	0.62	
Mission 2 Energy	19.0	16.1	26.3	W-Hr
Normalized Rank	0.85	1.00	0.61	

Totals	Waterjet	VTOL Tailsitter	Quadrotor Hybrid
Rank - Mission 1	0.80	1.00	0.62
Rank - Mission 2	0.85	1.00	0.61
Total Score	1.65	2.00	1.23

Experimental Testing

With the design phase completed, development turned to constructing and validating the physical vehicle. Subsystem experimental development was conducted in a closed pool on a number of test articles. These tests were designed to build towards and end with flight demonstration of a complete vehicle system.

Propulsion Testing

Water motor/propeller testing was conducted in a local swimming pool in nominally quiescent water. The apparatus shown on the right in figure 5 was used for this testing. The motor and propeller were mounted to the bottom of a fixed, vertical beam facing downward. At the top of the beam was a force sensor. The beam was lowered until the motor and propeller were both submerged. Wiring came up the beam to an ESC and RC (radio controller) receiver. A transmitter was used to control motor throttle. The motor used was a Hacker A-40 motor with an APC 9x4.5 propeller cut down to a diameter of 4.25 in (10.8 cm). Throttle was incremented up from 0% by 25%. Output force data is shown in figure 6. Before reaching 50% throttle, the ESC cut power to the motor. This was likely caused by the overcurrent safety on the ESC. Submerging a propeller designed to be used in air causes the motor to draw much more current than in air. As a result of this preliminary testing, a

gearbox was installed on the motor that reduced the gearing by 6.7:1.

Air motor testing was done in the NC State University wind tunnel as pictured on the left in figure 5. The motor used was a Hacker A-50 Motor with an APC 19x10 propeller. Two cases were run. One was a static-thrust test, the second was a cruise-thrust test. Figure 6 shows the results of thrust versus throttle setting. As can be seen in the plot the maximum static thrust produced is well above the 10 lbs (44 N) vehicle weight. This meets the requirements for thrust-to-weight ratio of greater than one. The thrust produced at cruise was measured in a 60 mph (31 m/s) freestream velocity which matches the design cruise speed.

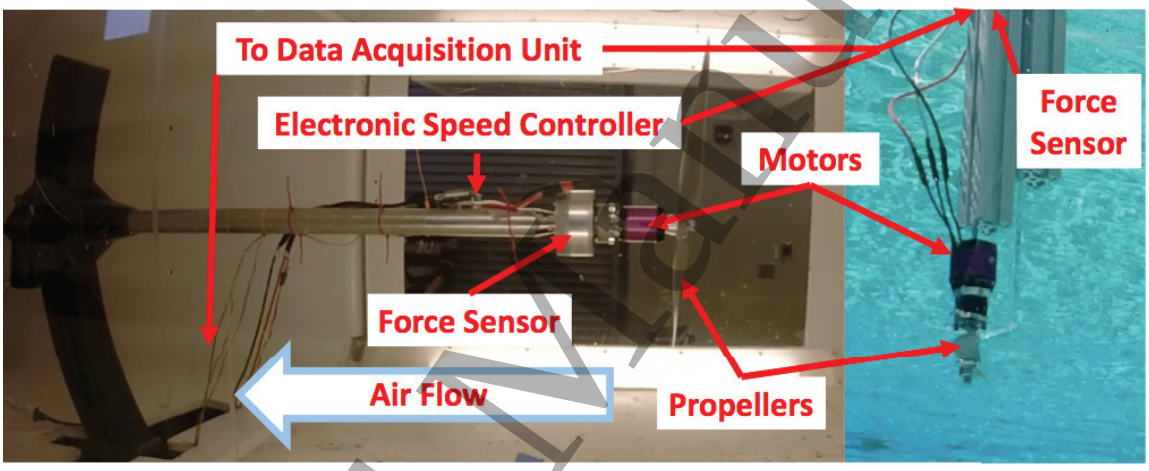

Figure 5. Air motor test setup on the left, water motor test setup on the right. The water motor force sensor, ESC, and Data Aquisition Unit are out of the frame and above the water.

Wing Construction & Draining Tests

The wing frame was built with a pultruded-carbon-fiber truss as a spar connecting waterjet-cut aluminum ribs. Three layers of bidirectional carbon fiber cloth were used for the upper and lower wing skins. The wing skins and wing frame were bonded together using HYSOL E-120HP epoxy. Wing structural sizing was performed by assuming a worst-case scenario whereby the vehicle plunges into the water nose first. A detailed analysis such as the numerical simulations by the Naval Research

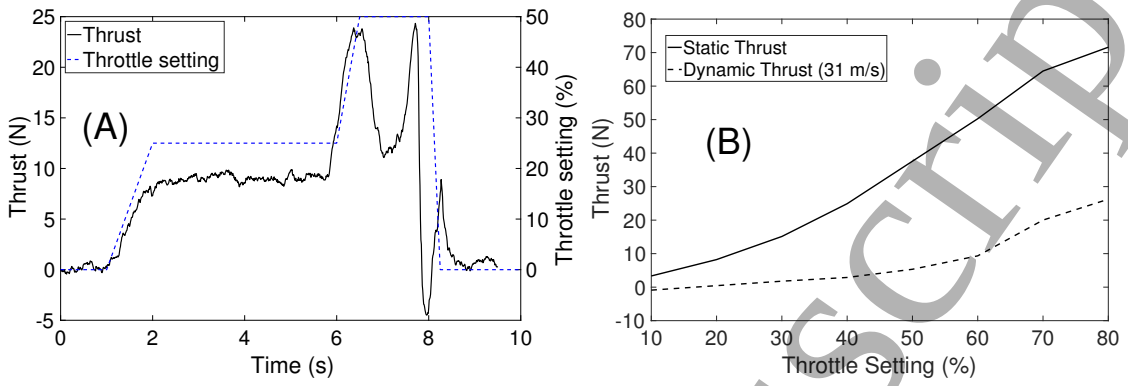

Figure 6. (a) Water motor testing. From 0 to 1 second, throttle was set to 0%. Between 2 and 6 seconds, throttle was set to 25%. At 6 seconds the throttle was set to 50%. The ESC cut off at 8 seconds. (b) Air motor testing in a wind tunnel. Maximum tested thrust occurred at 80% throttle for both cases.

Laboratory [14] would be needed to accurately design the airframe structure to efficiently handle the landing loads. However, the object of this work was to demonstrate the viability of this vehicle operational approach. Therefore, we modeled the entry as a vertical impact plunge dive as described by Abrate [37]. The idealized beam method was used to estimate the added structural weight required to survive this landing. Deceleration was modeled from Abrate [37],

$$\ddot{\xi} = \frac{\pi \rho_w (r - \xi)(-MU_i)^2}{(M + M_a)^3} \tag{13}$$

Where, $\ddot{\xi}$ is the acceleration of the leading edge of the wing relative to the water surface, r is the radius of the leading edge of the wing, and U_i is the impact velocity. The impact load was then estimated using Newton's Second Law of Motion and the given deceleration. The idealized beam method, as laid out by Megson [38], was then applied and iterated until a minimum-weight configuration was reached.

The plunge dive analysis was done at 7.72 m/s, which was the half the estimated stall speed of the aircraft. Applying equation (13) to the wing gave a maximum estimated impact load of 2.2kN per unit span, or about 3.2kN total. These loads roughly correspond to the results from the numerical solver used by the Naval Research Lab [14]. To alleviate landing loads of a nose-first landing, a strip of Kevlar was used to along the leading edge to absorb impact energy of the landing.

The upper skin employed a strip of kevlar fabric to act as a live hinge for the spoilerons. Two strips of kevlar were bonded to the leading edge to hold the upper and lower skins together at the leading edge. Servos were mounted to the aluminum ribs, and pushrods were run outside the wing structure. As a result of preliminary testing on a small section of the wing, a hydrophobic coating was found to not be necessary to achieve flight, and so was not included. Further analysis of the wing design and performance is presented in Stewart et al. [36].

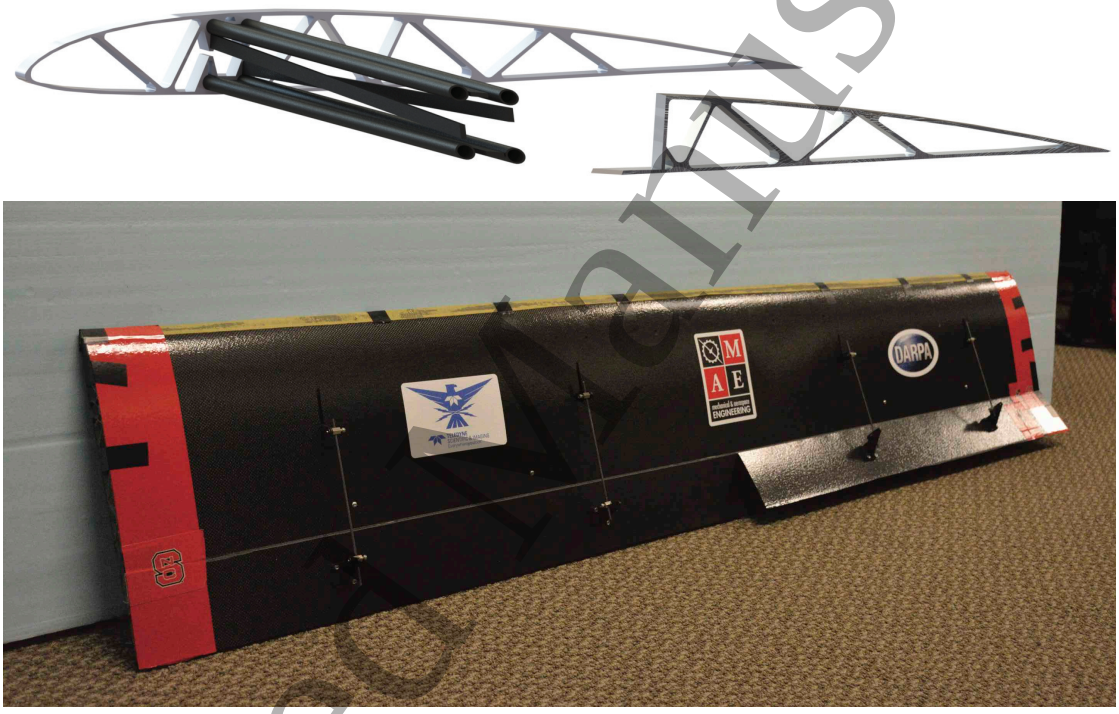

Figure 7. CAD rendering of wing truss structure (ribs separated from spar for clarity) and full scale wing photograph.

Full-Vehicle Underwater Operation

A prototype of the VTOL vehicle was built. An aluminum tube with a 3 in (7.6 cm) outer diameter was used for the fuselage, and a carbon-fiber tail boom was used to support the empennage. Aluminum tail surfaces were waterjet cut from 0.0625 in (1.6 mm) sheet Aluminum 2024. A PVC screw-on cap was used on the front to

allow access to the inside. The gross weight of the aircraft was 11 lbs (49 N). It included two motors, one sized for air operations and the other for water operation. The vehicle did not include an active buoyancy control device.

Matching the propulsion tests, the air motor used was a Hacker A-50 Motor with an APC 19x10 propeller. The water motor used was a Hacker A-40 motor with a gearbox was installed that reduced the gearing by 6.7:1. The water propeller was an APC 9x4.5 propeller cut down to a diameter of 4.25 in (10.8cm). The ESCs were Castle Phoenix Edge 75 and Castle Phoenix Edge 100 for air and water respectively. Both motors were powered by a single Thunderpower 6 cell 5000 mAh LiPo battery. As is pictured in figure 8, the ESCs, batteries, and a 72 MHz receiver were mounted in the dry section of the vehicle and the motors and propellers were positioned outside. Watertight cord grips were used to pass wiring from outside the vehicle to the inside. Three waterproof servos were mounted on the tail of the vehicle to actuate the elevators and rudder. Four more were used to actuate spoilerons on the wing.

Pool and Egress Testing

The vehicle was first used to demonstrate maneuverability underwater. ESC and motor thrust was verified to be adequate for submerged operation of this vehicle. Egress testing was conducted in the pool by tethering the aircraft to weights resting on the bottom of the pool with nylon safety lines. To ensure a slight positive buoyancy with a pitch up attitude, polystyrene closed cell foam was attached to the forward portion of the fuselage. These tests confirmed the vehicle could conduct the egress maneuver and gave the pilot practice performing the egress in a controlled environment. Video footage of the practice egress showed that the wing almost completely drained within an estimated 0.5 s after takeoff, as seen in figure 9. Furthermore, it was found that a considerable amount of down elevator was required to maintain vertical attitude during egress. This down elevator deflection was used to counter the moment from both the wing lift and the combined weight of the wing and water in the wing resulting from imperfect draining.

Demonstration of Full Aerial-Underwater Operation

A university-owned lake was used for water egress and flight testing. As with the egress testing, the buoyancy trim was set such that, when unpowered, the aircraft

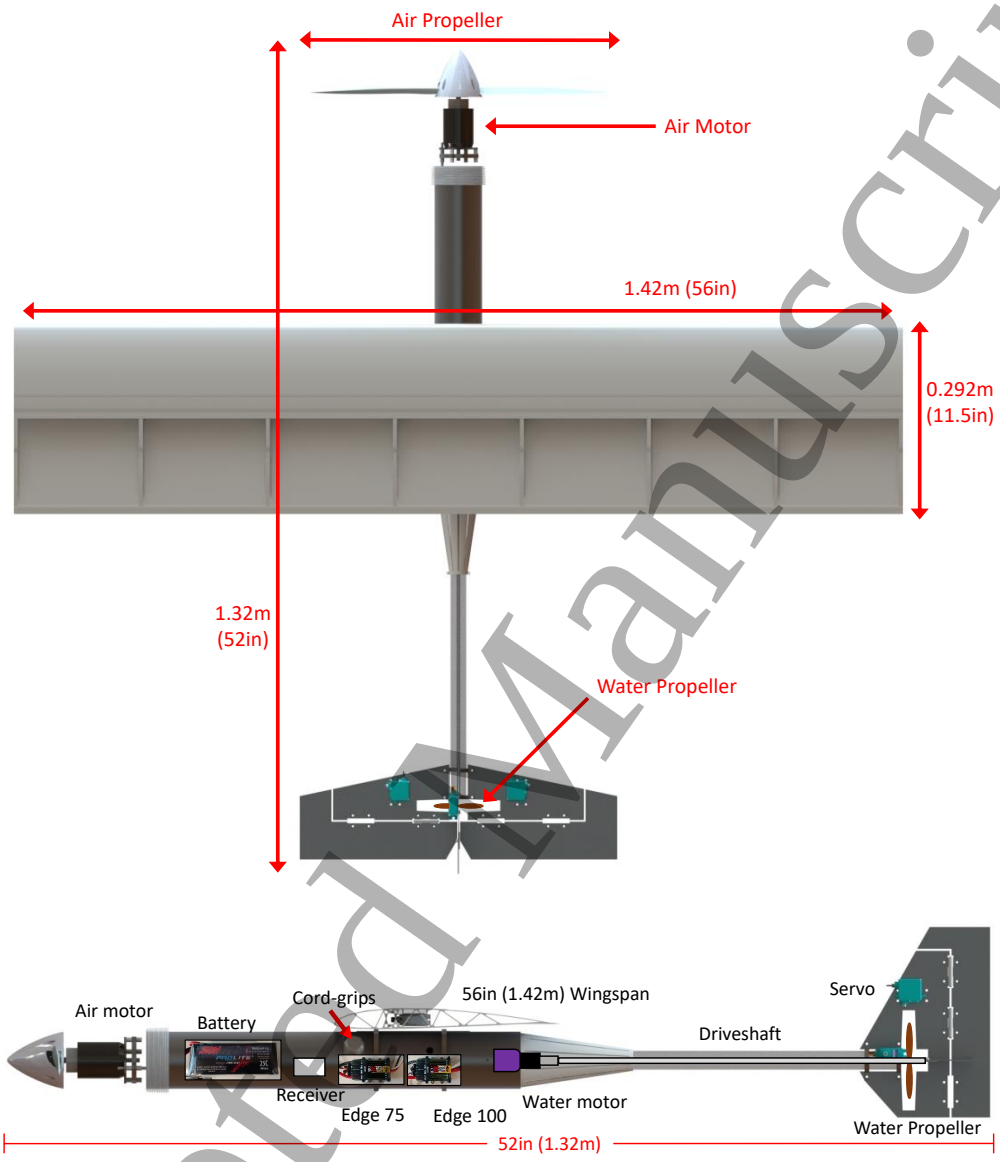

Figure 8. Full vehicle CAD rendering as well as a cutaway of the vehicle. The section housing the purple water motor and the wing are both floodable sections of the vehicle.

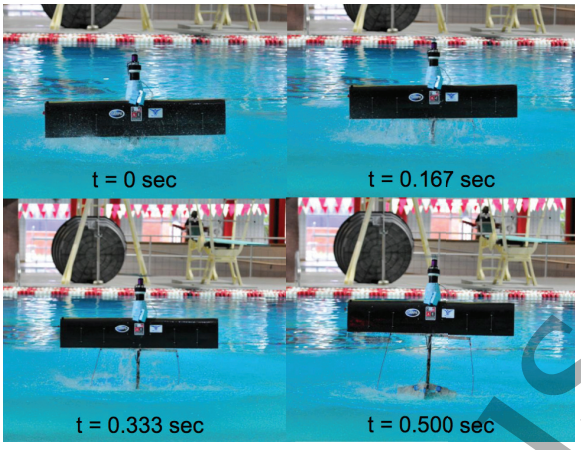

Figure 9. Egress testing in pool illustrating wing draining performance.

would suspend in a pitched-up orientation with the nose of the vehicle just visible at the water's surface. On takeoff the vehicle conducted a complete uncontrolled roll while in the vertical operating mode. This was a result of a large amount of propeller torque. In response to this torque, the pilot applied roll control by deflecting the spoileron control surfaces. This command however, closed that side of the wing, preventing water from draining on one side, which compounded with the rolling moment from the motor torque overwhelming the control power of the spoilerons. Nevertheless, the vehicle was able to complete the takeoff and reach an estimated altitude of 200 ft (61 m) AGL. While at altitude in air, the pitchup to vertical orientation for landing was practiced. It was observed that the vehicle had a tendency to enter an inverted flat spin while performing the maneuver. As a result, the landing procedure was modified to be a stall-splash maneuver similar to the landing pattern of the waterjet vehicle concept. After a few successful landings, it was determined that this type of landing is adequate for calm sea states. Once landed, the vehicle swam in the water back to shore on the surface of the water. All mission demonstrations began in the water, transitioned to air, and returned to the water. On numerous occasions, short hops whereby the vehicle egressed and returned to the water were conducted before a longer flight. This demonstrates the vehicle's ability to conduct multiple egresses and ingresses within one mission. Figure 10 shows images of the vehicle egressing, in flight, landing, and cruising on the water surface. A total of 11 minutes, 23 seconds of flight time was recorded over 3 flights.

No on board data logging was conducted during these proof-of-concept flights.

In between flights, the vehicle was inspected for damage. The wing structure received minimal damage over the course of the flight testing regimen. Mostly the wing damage was concentrated on the Kevlar live hinge which gradually tore due to tips strikes during imperfect landings. Future vehicles will incorporate a continuous fiber hinge into the carbon fiber to address this issue. Part of the reason for the lack of critical wing damage over the course of flight tests conducted was due to propeller-first impacts, which would dissipate a large amount of energy before the wing entered the water. This resulted in more damaged propellers than damaged wings. Future vehicles will address this with the use of folding propellers to reduce bending loads at impact.

Conclusions

This paper has outlined the design process for the development of a seabird inspired fixed-wing, air-water vehicle capable of multiple transitions between air and water. Multiple subsystem designs, drawing from the natural world have been investigated. This vehicle uses separate propulsion systems for air and water like web-footed waterfowl and counteracts positive buoyancy by swimming downward like seabirds to complete a mission inspired by the hunting expeditions of the common murre. After analysis of three vehicle concepts, the tailsitter VTOL configuration aircraft was selected for further development and demonstrated operations both underwater and in air. The proof of concept vehicle has demonstrated a full cycle of water egress, air flight, water ingress, and underwater locomotion. With the completion of these four tasks, it has been demonstrated that the design developed here was able to complete all four required tasks for a hybrid UAV-UUV. Table 4 lists the bioinspired features present and demonstrated on the prototype vehicle. Additional work by Weisler et al, implements onboard data logging on a subsequent version of the vehicle and characterized the vehicle handling and performance [39].

The subsystems used in the design are all scalable, allowing this design to be used for many different hybrid UAV-UUV vehicles in the future. Cruise speed, for example, is a function of wing loading, parasitic drag, and wing efficiency, all three of which scale well. Scaling the wing up and increasing span will increase aerodynamic efficiency and therefore will result in longer range and higher endurance in the air. Overall, thrust can be increased through the use of larger motors and batteries, which

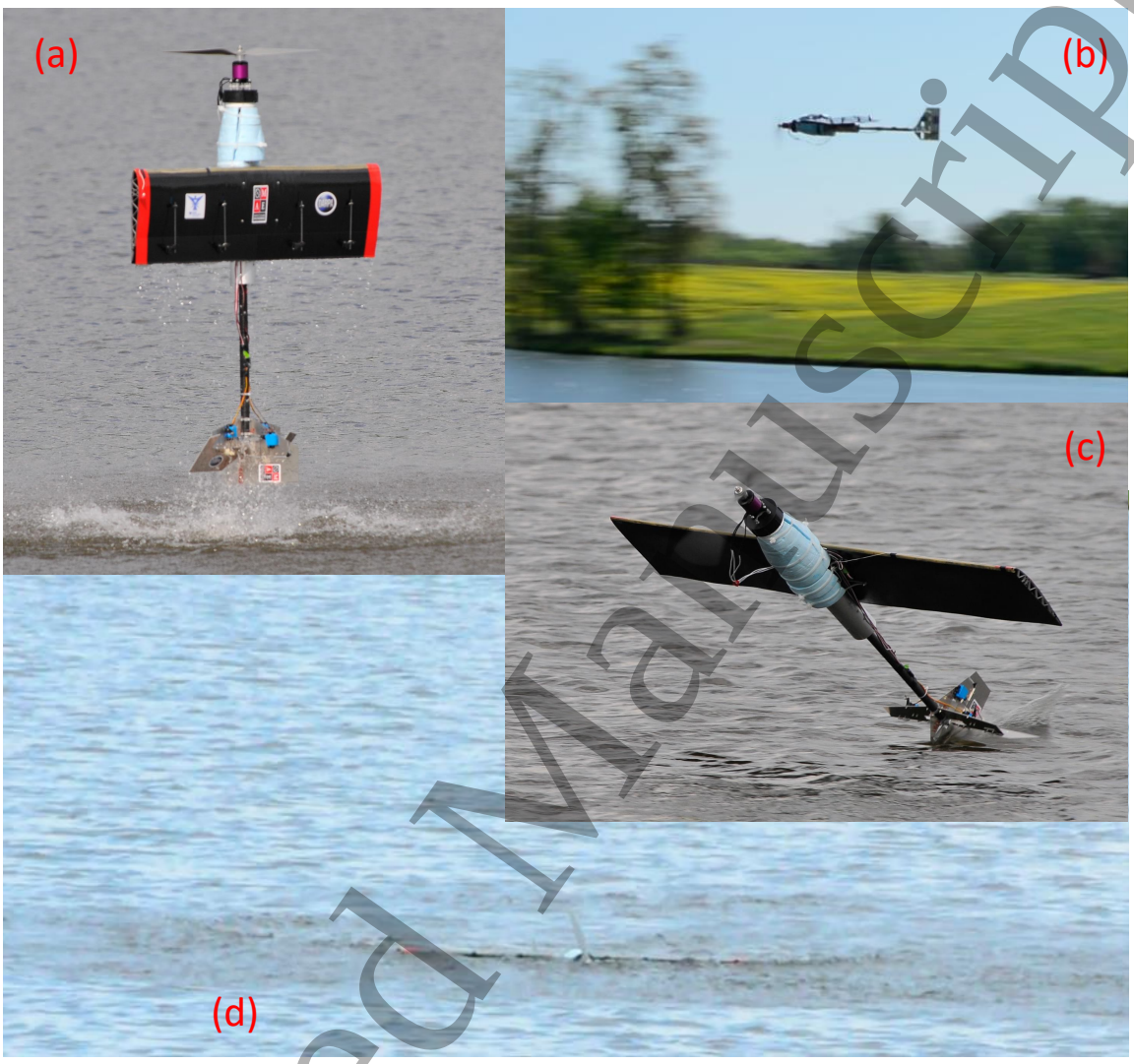

Figure 10. (a) Vehicle egress. Visible here is the down elevator required to maintain vertical orientation during takeoff; (b) Air flight; (c) Vehicle ingress; (d) Surface cruise back to shore.

Table 4. Bioinspirated Concepts on Vehicle

Inspiration	Concept	Implementaion
Common murre	Hunting expedition including multiple cycles of flight/swim/flight	Vehicle demonstrated multiple domain transitions in a single mission
Common murre	Submerged ascent / descent via swimming	Vehicle both ascended and descended under electric motor power in controlled pool tests
Ducks	Separate propulsion systems for use in air or water	The vehicle utilizes two motor / propeller combinations, one for and air and one for water

will allow for a payload increase. Additional improvements can also be made, such as reducing the weight of solid aluminum tail surfaces, increasing the roll control authority, addition of autonomy, and implementation of a buoyancy control device.

Acknowledgements

This material is based upon work supported by SSC Pacific under Contract No. N66001-14-C-4008 (DARPA primary sponsor).

K. Peters was partially supported by the National Science Foundation, while working at the Foundation. Any opinion, finding, and conclusions or recommendations expressed in this material are those of the author and do not necessarily reflect the views of the National Science Foundation.

References

[1] N. Kokubun, T. Yamamoto, N. Sato, Y. Watanuki, A. Will, A. Kitaysky, and A. Takahashi. Foraging segregation of two congeneric diving seabird species breeding on st. george island, bering sea. *Biogeosciences*, 13:2579–2591, 2016.

[2] G. Hunt, Z. Eppley, and D. Schneider. Reproductive performance of seabirds: The importance of population and colony size. *The Auk*, 103(2):306–317, 1986.

[3] A. Hedd, P. Regular, W. Montevecchi, A. Buren, C. Burke, and D. Fifield. Going deep: common murres dive into frigid water for aggregated, persistent and slow-moving capelin. *Mar Biol*, 156:741–751, 2009.

[4] R. Siddall and M. Kovac. Launching the aquamav: Bioinspired design for aerial-aquatic robotic platforms. *Bioinspiration & Biomimetics*, 9(3):031001, 2014.

[5] R. M. Alexander. One price to run, swim or fly? *Nature*, 397:651–653, February 1999.

[6] J. Davenport. How and why do flying fish fly? *Reviews in Fish Biology and Fisheries*, 4:184–214, 1994.

[7] G.T. Reels and R. Dow. Underwater oviposition behavior in two species of euphaea in borneo and hong kong. *International journal of odonatology (Odonata : Euphaeidae)*, 9:197–204, 2006.

[8] R. Siddall, M. de Launay, and M. Kovac. A water jet thruster for an aquatic micro air vehicle. In *IEEE International Conference on Robotics and Automation (ICRA)*, pages 3979–3985. Institute of Electrical and Electronics Engineers, May 2015.

[9] R. Siddall and M. Kovac. Fast aquatic escape with a jet thruster. *IEEE/ASME Transactions on Mechatronics*, PP(99):1–1, 2016.

[10] K. Low, T. Hu, S. Mohammed, J. Tangorra, and M. Kovac. Perspectives on biologically inspired hybrid and multi-modal locomotion. *Bioinspiration & Biomimetics*, 10, 2015.

[11] R. Siddall, A. Ortega, and M. Kovac. Wind and water tunnel testing of a morphing aquatic micro air vehicle. *Interface Focus*, 7(1), 2016.

[12] Naval Research Lab. Navy launches uav from submerged submarine. [Online]. Available: http://www.nrl.navy.mil/media/news-releases/2013/navy-launches-uav-from-submerged-submarine.

[13] T. Young. Design and testing of an air-deployed unmanned underwater vehicle. In *14th AIAA Aviation Technology, Integration, and Operations Conference*. American Institute of Aeronautics and Astronautics, 2014.

[14] R. Ramamurti, J. Geder, D. Edwards, and T. Young. Computational studies for the development of a hybrid uav/uuv. In *AIAA AVIATION Forum*. AIAA, June 2015.

[15] R. Goddard and J. Eastgate. Submersible aircraft concept design study. In *11th International Conference on Fast Sea Transportation*, pages 813–820, September 2011.

[16] G.L. Crouse Jr. Conceptual design of a submersible airplane. In *48th AIAA Aerospace Sciences Meeting Including the New Horizons Forum and Aerospace Exposition*, January 2010.

[17] P. Drews-Jr, A. Alves Neto, and M. Fernando Montenegro Campos. Hybrid unmanned aerial underwater vehicle: Modeling and simulation. In *2014 IEEE/RSJ International Conference on Intelligent Robots and Systems*, pages 4637–4642. IEEE, September 2014.

[18] M. Maia, P. Soni, and F. Diez-Garias. Demonstration of an aerial and submersible vehicle capable of flight and underwater navigation with seamless air-water transition. Available here: http://arxiv.org/pdf/1507.01932.pdf.

[19] K. Elliot, G. Davoren, and A. Gaston. The influence of buoyancy and drag on the dive behaviour of an artic seabird, the thick-billed murre. *Canadian Journal of Zoology*, 85:353–361, 2007.

[20] M. MacLeod and M. Bryant. Dynamic modeling, analysis, and testing of a variable buoyancy system for unmanned multidomain vehicles. *IEEE Journal of Oceanic Engineering*, 42(3):511 – 521, August 2016.

[21] J. R. Lovvorn and D. R. Jones. Biomechanical conflicts between adaptions for diving and aerial flight in estuarine birds. *Estuaries Coasts*, 17(1A):62–75, 1994.

[22] M. Ogilvie and D. Wallace. Field identification of grey geese. *British Birds*, 68:57–67, 1975.

[23] Y. Liu, X. Chen, and J. Xin. Hydrophobic duck feathers and their simulation on textile substrates for water repellent treatment. *Bioinspiration and Biomimetics*, 3, 2008.

[24] L. Feng, S. Li, Y. Li, H Li, L. Zhang, J. Zhai, Y. Song, B. Liu, L. Jiang, and D. Zhu. Super-hydrophobic surfaces: From natural to artificial. *Advanced Materials*, 14(24), 2002.

[25] E. Anderson and M. Demont. The locomotory function of the fins in the squid loligo pealei. *Marine and Freshwater Behaviour and Physiology*, 38(3):169–189, 2005.

[26] Farhan Gandhi. Centrifugal force actuated variable span helicopter rotor. U.S. Patent num US8152466 B2, April 2009.

[27] Y. Tan, R. Siddall, and M. Kovac. Efficient aerial-aquatic locomotion with a single propulsion system. *IEEE Robotics and Automation Letters*, 2(3):1304 – 1311, July 2017.

[28] Y. Chen, H. Wang, E. Helbling, N. Jafferis, R. Zufferey, A. Ong, K. Ma, N. Gravish, P. Chirarattananon, M. Kovac, and R. Wood. A biologically inspired, flapping-wing, hybrid aerial-aquatic microrobot. *Science Robotics*, 2, October 2017.

[29] R. Siddall, G. Kennedy, and M. Kovac. High-power propulsion strategies for aquatic take-off in robotics. In *Robotics Research: 17th International Symposium ISRR*. Springer International Publishing, 2015.

[30] Latitude Engineering. Hybrid quadrotor technology. https://latitudeengineering.com/products/hq/, June 2017.

[31] Aerovel. Flexrotor unmanned aerial system. http://aerovelco.com/flexrotor/, June 2017.

[32] M. Drela. Avl. Available here: http://web.mit.edu/drela/Public/web/avl/.

[33] M. Drela. Xfoil. Available here: http://web.mit.edu/drela/Public/web/xfoil/.

[34] B. McCormick. *Aerodynamics, Aeronautics, and Flight Mechanics*. John Wiley & Sons, LTD, 2nd edition edition, 1995.

[35] S. Hoerner. *Fluid Dynamic Drag*. Hoerner Fluid Dynamics, 2nd edition edition, 1992.

[36] W. Stewart, W. Weisler, M. Bryant, K. Peters, and M. Anderson. Dynamic modeling of passively draining structures for aerial-aquatic unmanned vehicles. Submitted to Journal of Oceanic Engineering.

[37] S. Abrate. Hull slamming. *Applied Mechanics Review*, 64, November 2011.

[38] T. Megson. *Aircraft Structures for Engineering Students*. Elsevier, 2007.

[39] W. Weisler, W. Stewart, M. Bryant, A. Gopalarathnam, and K. Peters. Testing and

characterization of a fixed wing cross-domain unmanned vehicle operating in aerial and underwater environments. *Journal of Oceanic Engineering*, PP(99):1–14, 2017.